

Supplemental Information

Serine ADP-ribosylation in *Drosophila* provides insights into the evolution of reversible ADP-ribosylation signaling

Pietro Fontana^{1,2,3,*}, Sara C. Buch-Larsen^{4,*}, Osamu Suyari^{1,*}, Rebecca Smith¹, Marcin J. Suskiewicz^{1,5}, Kira Schützenhofer¹, Antonio Ariza^{1,6}, Johannes Gregor Matthias Rack^{1,7}, Michael L. Nielsen⁴, Ivan Ahel¹

¹ Sir William Dunn School of Pathology, University of Oxford, South Parks Road, Oxford, OX1 3RE, UK.

² Department of Biological Chemistry and Molecular Pharmacology, Harvard Medical School, Boston, MA, USA.

³ Program in Cellular and Molecular Medicine, Boston Children's Hospital, Boston, MA, USA.

⁴ Proteomics program, Novo Nordisk Foundation Center for Protein Research, Faculty of Health and Medical Sciences, University of Copenhagen, Blegdamsvej 3B, 2200 Copenhagen, Denmark.

⁵ Current address: Centre de Biophysique Moléculaire, UPR4301 CNRS, rue Charles Sadron, CEDEX 2, F-45071 Orléans, France.

⁶ Current address: School of Biosciences, University of Sheffield, Western Bank, Sheffield, S10 2TN, UK.

⁷ Current address: MRC Centre for Medical Mycology, School of Biosciences, University of Exeter, Geoffrey Pope Building, Exeter, EX4 4QD, UK.

*These authors contributed equally.

Correspondence to:

Ivan Ahel (ivan.ahel@path.ox.ac.uk)

Michael L. Nielsen (michael.lund.nielsen@cpr.ku.dk)

Johannes G. M. Rack (j.rack@exeter.ac.uk)

Antonio Ariza (a.ariza@sheffield.ac.uk)

Supplemental Table 1. PARP sequences utilized to analyse automodification domain.

species				
binominal name	common name ^a	accession ^b	ARH3 homologue present	HPF1 with PBZ
Insecta				
<i>Acromyrmex heyeri</i>	Formiga-de-monte-vermelha	KAG5332370	yes	yes
<i>Aphis gossypii</i>	Cotton aphid	XP_027836345	no	yes
<i>Apis mellifera</i>	Honey bee	XP_624477	yes	yes
<i>Athalia rosae</i>	Coleseed sawfly	XP_012253348	yes	yes
<i>Bemisia tabaci</i>	Silverleaf whitefly	CAH0393176	yes	yes
<i>Blattella germanica</i>	German cockroach	PSN54639	yes	yes
<i>Bombyx mori</i>	Domestic silk moth	XP_004926518	no	yes
<i>Cimex lectularius</i>	Bed bug	XP_014252361	yes	yes
<i>Cloeon dipterum</i>	Pond Olive	CAB3383108	no	no ^c
<i>Cryptotermes secundus</i>	<i>n.a.</i>	XP_023719718	yes	yes
<i>Danaus plexippus plexippus</i>	Monarch Butterfly	OWR47253	no	yes
<i>Diabrotica virgifera virgifera</i>	Western corn rootworm	XP_028137801	yes	yes
<i>Drosophila melanogaster</i>	Fruit fly	NP_001104452	no	yes
<i>Formica exsecta</i>	Narrow-headed ant	XP_029670266	yes	yes
<i>Frankliniella occidentalis</i>	Western flower thrips	XP_026271855	yes	yes
<i>Galleria mellonella</i>	Greater wax moth	XP_026751130	no	yes
<i>Harmonia axyridis</i>	Halloween beetle	XP_045461901	yes	yes
<i>Homalodisca vitripennis</i>	Glassy-winged sharpshooter	XP_046681652	yes	yes
<i>Hyposmocoma kahamanoa</i>	<i>n.a.</i>	XP_026328627	no	yes
<i>Ignelater luminosus</i>	Cucubano	KAJ2885554	yes	yes
<i>Ischnura elegans</i>	Blue-tailed damselfly	XP_046383121	yes	yes
<i>Lasius niger</i>	Black garden ant	KMQ98224	yes	yes
<i>Monomorium pharaonis</i>	Pharaoh ant	XP_012538492	yes	yes
<i>Musca domestica</i>	Housefly	XP_005175605	no	yes
<i>Myzus persicae</i>	Green peach aphid	XP_022178738	no	yes
<i>Ooceraea biroi</i>	Clonal raider ant	XP_011334668	yes	yes
<i>Photinus pyralis</i>	Common eastern firefly	XP_031330927	yes	yes
<i>Schistocerca americana</i>	American grasshopper	XP_046979867	yes	yes
<i>Sipha flava</i>	Yellow sugarcane aphid	XP_025410796	no	yes
<i>Sitophilus oryzae</i>	Rice weevil	XP_030752809	yes	yes
<i>Thrips palmi</i>	Melon thrips	XP_034248574	no	yes
<i>Timema tahoe</i>	<i>n.a.</i>	CAD7458304	yes	yes
<i>Tribolium castaneum</i>	Red flour beetle	EFA00829	yes	yes
<i>Tribolium madens</i>	Black flour beetle	XP_044269707	yes	yes
<i>Trichoplusia ni</i>	Cabbage looper	XP_026729426	no	yes
<i>Zerene cesonia</i>	Dogface butterfly	XP_038210310	no	yes
Mammalia				
<i>Balaenoptera musculus</i>	Blue whale	XP_036723058	yes	no
<i>Homo sapiens</i>	Human	NP_001609	yes	no
<i>Orycteropus afer afer</i>	Aardvark	XP_007935170	yes	no

^anot applicable (*n.a.*) designates species with no common name

^bGenBank accession number

^cHPF domain is predicted to be part of a multidomain protein (GenBank CAB3360198) with unique architecture. Our analysis of the genomic region revealed the presence of a potential PBZ coding region upstream of the HPF domain.

Supplemental Table 2. Data collection and refinement statistics (molecular replacement)

	<i>d</i> Parg ^a (PDB 8ADK)	<i>d</i> Parg:PDD00017273 ^a (PDB 8ADJ)
Data collection		
Space group	<i>P</i> 2 ₁	<i>P</i> 2 ₁
Cell dimensions		
<i>a</i> , <i>b</i> , <i>c</i> (Å)	93.43, 115.62, 122.91	93.39, 115.90, 123.27
α , β , γ (°)	90.00, 90.00, 112.21	90.00, 90.00, 112.21
Resolution (Å) ^b	58.95 – 2.48 (2.53 – 2.48)	59.02 – 2.51 (2.58 – 2.51)
<i>R</i> _{sym} or <i>R</i> _{merge} ^b	0.087 (1.116)	0.133 (2.020)
<i>I</i> / σ ^b	9.6 (1.1)	9.6 (1.1)
Completeness (%) ^b	99.7 (99.3)	100.0 (100.0)
Redundancy ^b	3.3 (3.4)	6.7 (6.7)
Refinement		
Resolution (Å)	2.47	2.51
No. reflections	85715	83225
<i>R</i> _{work} / <i>R</i> _{free}	0.177 / 0.228	0.183 / 0.223
No. atoms		
Protein	12576	12521
Ligand/ion	63/3	165/3
Water	277	201
<i>B</i> -factors		
Protein	70.57	72.70
Ligand/ion	85.17/75.39	79.27/81.75
Water	51.91	55.00
R.m.s. deviations		
Bond lengths (Å)	0.0123	0.0092
Bond angles (°)	1.895	1.681

^aData were collected from a single crystal^bValues in parentheses are for highest-resolution shell.

Supplemental Table 3. PARG sequences utilized for multiple sequence alignment.

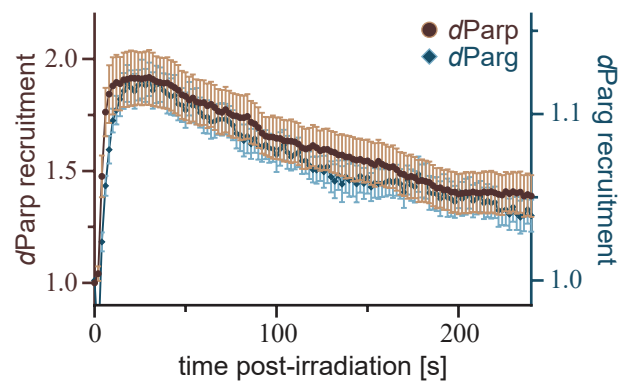
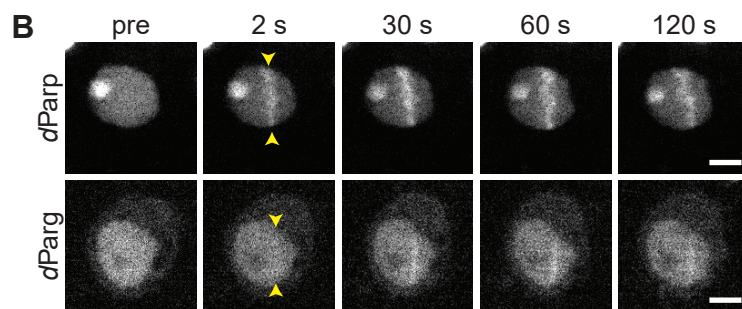
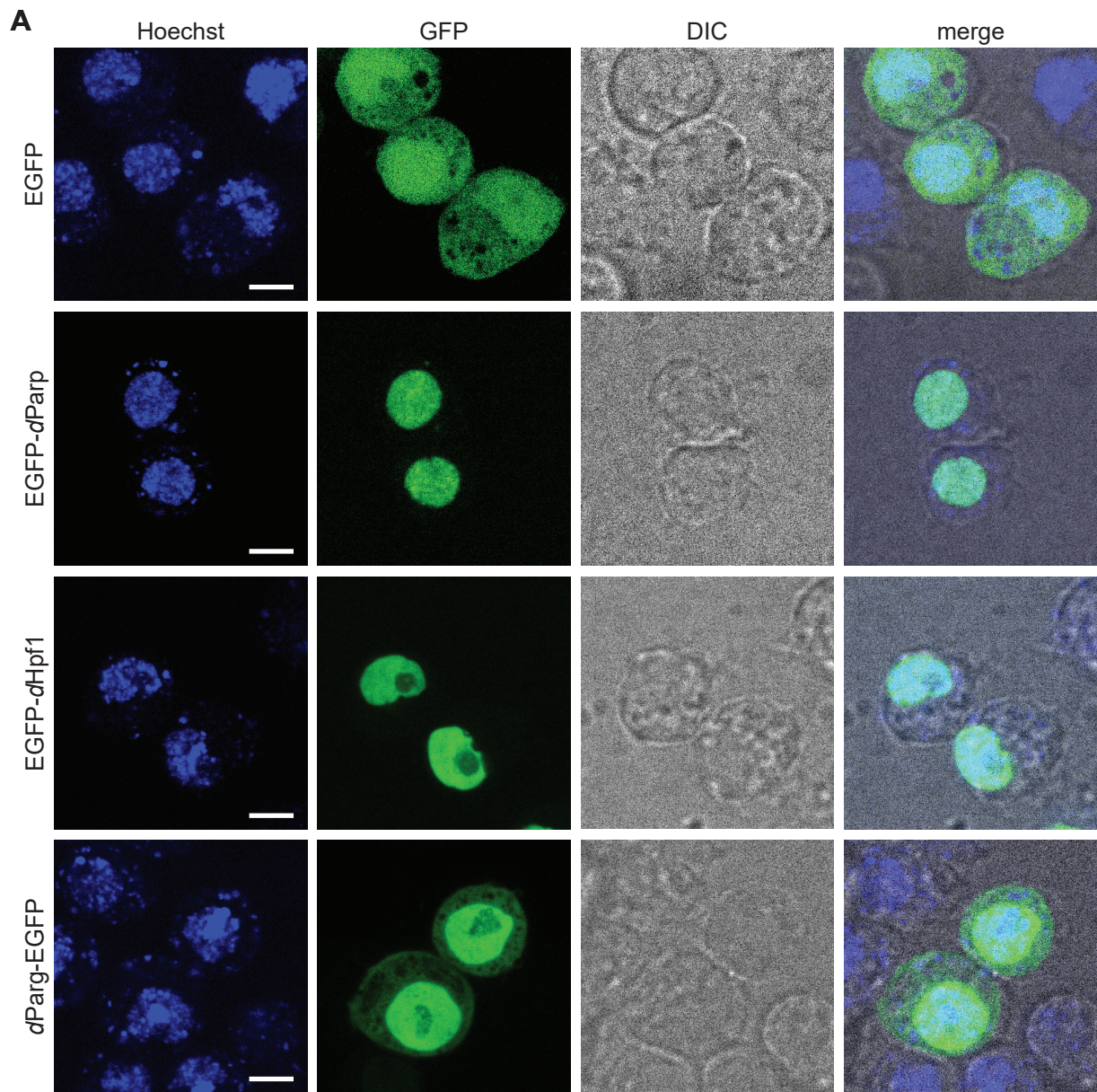
binominal name	species common name^a	accession number^b
<i>Caenorhabditis elegans</i>	<i>n.a.</i>	NP_001023135 ^c
<i>Caenorhabditis elegans</i>	<i>n.a.</i>	NP_501496 ^d
<i>Drosophila bunnanda</i>	<i>n.a.</i>	KAH8234568
<i>Drosophila melanogaster</i>	Fruit fly	NP_001245511
<i>Felis catus</i>	Domestic cat	XP_011285559
<i>Homo sapiens</i>	Human	NP_003622
<i>Loa loa</i>	Eye worm	XP_020303580
<i>Monosiga brevicollis</i> MX1	<i>n.a.</i>	XP_001748857
<i>Mus musculus</i>	Mouse	NP_036090
<i>Musca domestica</i>	House fly	XP_005174952
<i>Tetrahymena thermophila</i>	<i>n.a.</i>	XP_001013101
<i>Vombatus ursinus</i>	Common wombat	XP_027715098
<i>Zeugodacus cucurbitae</i>	Melon fly	XP_011177346

^anot applicable (*n.a.*)

^bGenBank accession number

^cSequence of PARG1

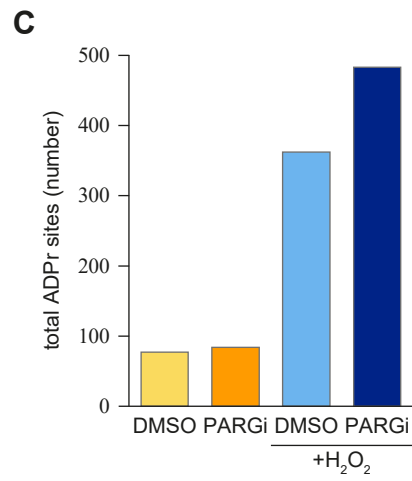
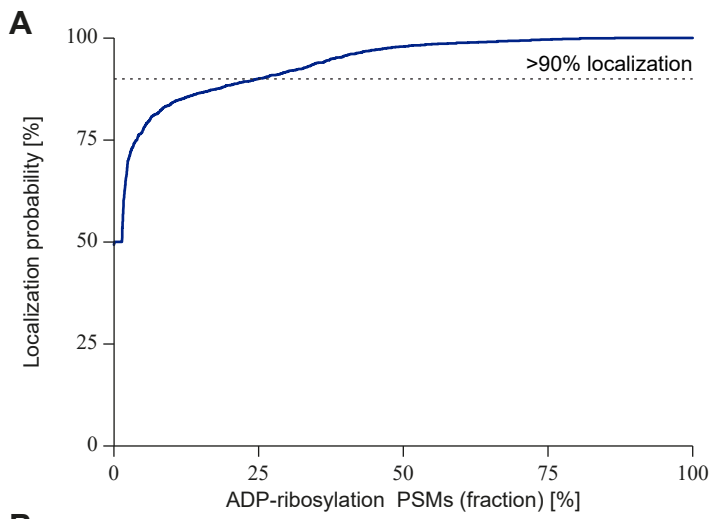
^dSequence of PARG2



Supplemental Figure 1. Subcellular localisation of the *Drosophila* DDR-ADPr enzymes.

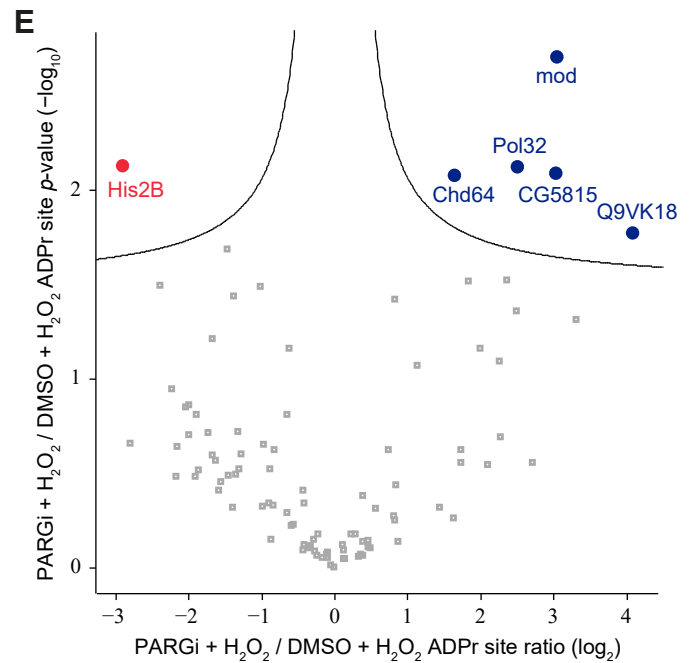
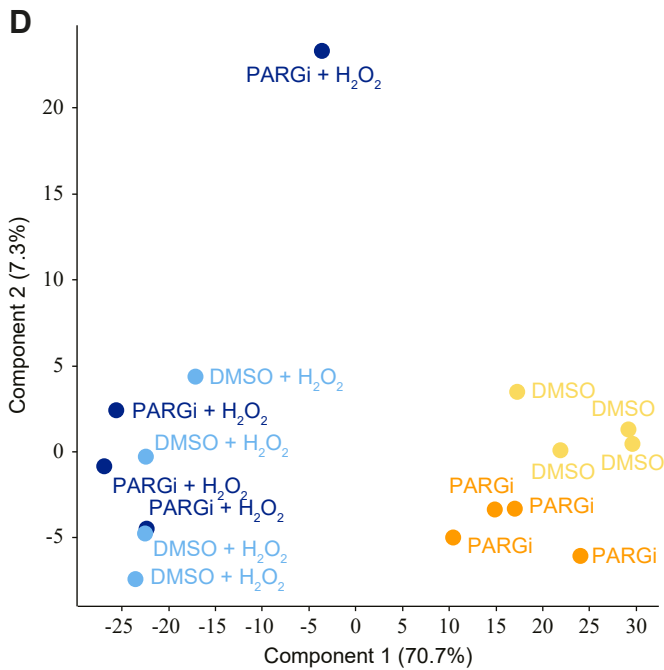
(A) Representative images of EGFP, EGFP-*d*Parp, EGFP-*d*Hpf1 and *d*Parg-EGFP expressed in *Drosophila* SR2⁺ cells. Hoechst is used to indicate localisation of the nucleus. Scale bar, 2 μ m. Sites of irradiation are indicated by yellow arrows. The experiment was repeated independently three times with similar results.

(B) Representative images (top) and kinetics (bottom) of EGFP-*d*Parp and *d*Parg-EGFP recruitment to sites of DNA damage induced by 405 nm laser irradiation, in *Drosophila* S2R⁺ cells. Scale bar, 2 μ m. Data from B are a representative of 3 independent replicates where data were collected from 16-25 cells per condition and represent normalised mean values \pm SEM.



B

	DMSO + H ₂ O ₂				DMSO				PARGi + H ₂ O ₂				PARGi				
	R1	R2	R3	R4	R1	R2	R3	R4	R1	R2	R3	R4	R1	R2	R3	R4	
DMSO + H ₂ O ₂	R1		0.90	0.58	0.88	0.49	0.58	0.51	0.74	0.73	0.83	0.54	0.82	0.65	0.72	0.65	0.58
	R2	0.90		0.78	0.89	0.80	0.78	0.76	0.82	0.61	0.93	0.78	0.91	0.86	0.89	0.86	0.77
	R3	0.58	0.78		0.57	1.00	1.00	1.00	0.85	0.37	0.94	0.87	0.92	0.95	0.90	0.88	0.99
	R4	0.88	0.89	0.57		0.51	0.56	0.53	0.80	0.62	0.78	0.64	0.79	0.63	0.72	0.68	0.58
DMSO	R1	0.49	0.80	1.00	0.51		1.00	1.00	0.85	0.36	0.93	0.97	0.91	0.99	0.95	0.95	0.99
	R2	0.58	0.78	1.00	0.56	1.00		1.00	0.84	0.39	0.94	0.85	0.91	0.96	0.92	0.91	0.98
	R3	0.51	0.76	1.00	0.53	1.00	1.00		0.84	0.30	0.93	0.89	0.91	0.95	0.90	0.89	0.98
	R4	0.74	0.82	0.85	0.80	0.85	0.84	0.84		0.56	0.89	0.80	0.90	0.81	0.83	0.81	0.85
PARGi + H ₂ O ₂	R1	0.73	0.61	0.37	0.62	0.36	0.39	0.30	0.56		0.58	0.29	0.60	0.38	0.47	0.39	0.37
	R2	0.83	0.93	0.94	0.78	0.93	0.94	0.93	0.89	0.58		0.85	0.99	0.93	0.93	0.89	0.93
	R3	0.54	0.78	0.87	0.64	0.97	0.85	0.89	0.80	0.29	0.85		0.82	0.87	0.86	0.86	0.86
	R4	0.82	0.91	0.92	0.79	0.91	0.91	0.91	0.90	0.60	0.99	0.82		0.88	0.88	0.85	0.92
PARGi	R1	0.65	0.86	0.95	0.63	0.99	0.96	0.95	0.81	0.38	0.93	0.87	0.88		0.99	0.96	0.94
	R2	0.72	0.89	0.90	0.72	0.95	0.92	0.90	0.83	0.47	0.93	0.86	0.88	0.99		0.98	0.91
	R3	0.65	0.86	0.88	0.68	0.95	0.91	0.89	0.81	0.39	0.89	0.86	0.85	0.96	0.98		0.91
	R4	0.58	0.77	0.99	0.58	0.99	0.98	0.98	0.85	0.37	0.93	0.86	0.92	0.94	0.91	0.91	



Supplemental Figure 2. Mass spectrometric identification of ADPr sites in S2R+ cells.

(A) Localization probability distribution of identified ADPr peptide-spectrum matches (PSMs). The dashed line visualizes the cutoff of >90% localization probability that was used.

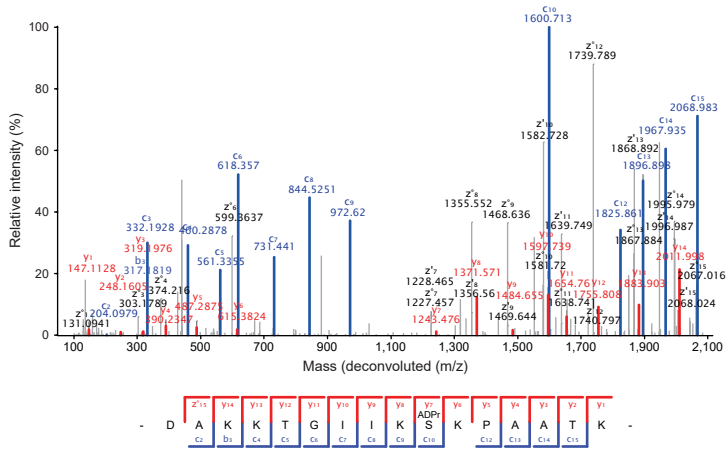
(B) Table with all Pearson correlations between different replicates and different conditions.

(C) Histogram visualizing the total number of ADPr sites identified and localized in the four different conditions.

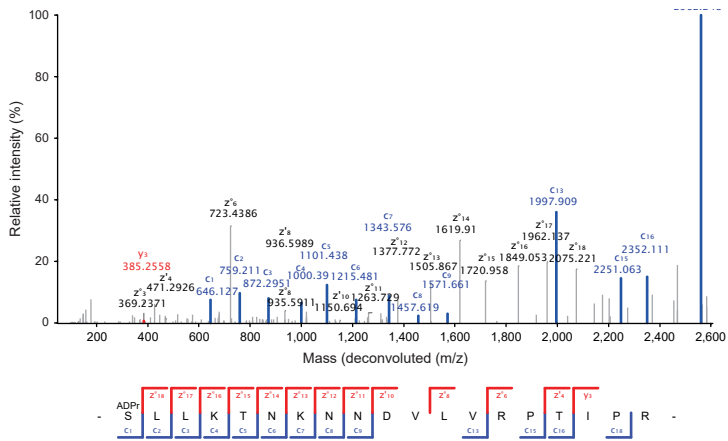
(D) Principal component analysis indicating the highest degree of variance between sample conditions.

(E) Volcano plot analysis visualizing the dynamics of PARGi-treated ADPr sites compared to DMSO-treated ADPr sites under DNA damage. Significance was determined via two-tailed Student's t-testing with a false discovery rate (FDR) of 0.05, s_0 of 0.1, and 2,500 rounds of randomization. ADPr sites significantly upregulated by PARGi treatment are depicted in blue, ADPr sites significantly upregulated upon DMSO treatment are depicted in red, and ADPr sites not significantly regulated are shown in grey.

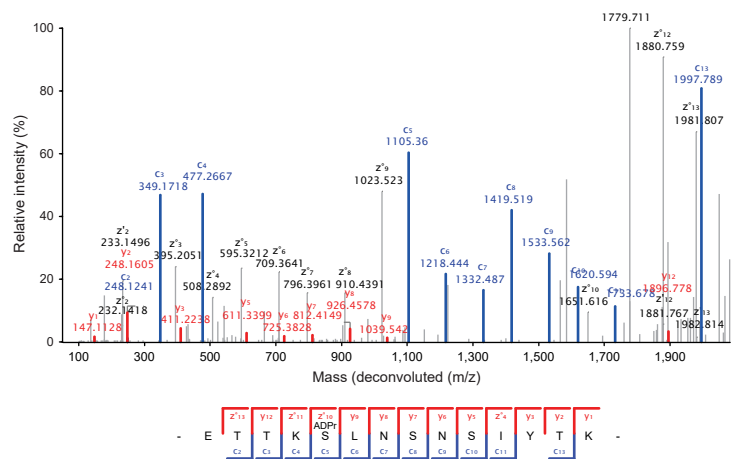
A dH1 S199mar



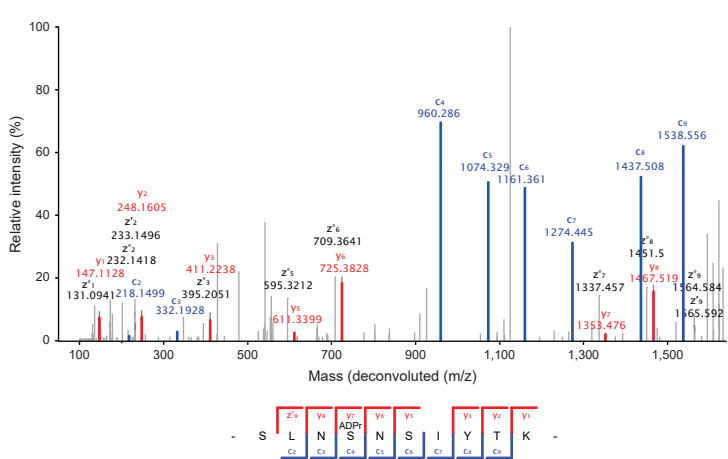
B dParp S362mar



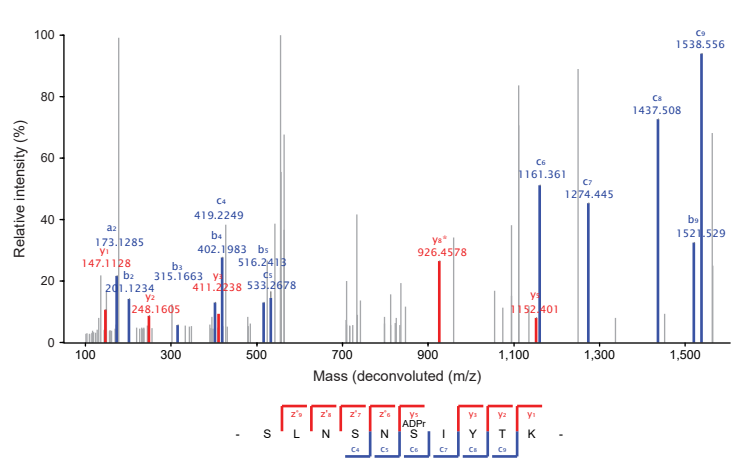
C dParp S491mar



D dParp S494mar



E dParp S496mar

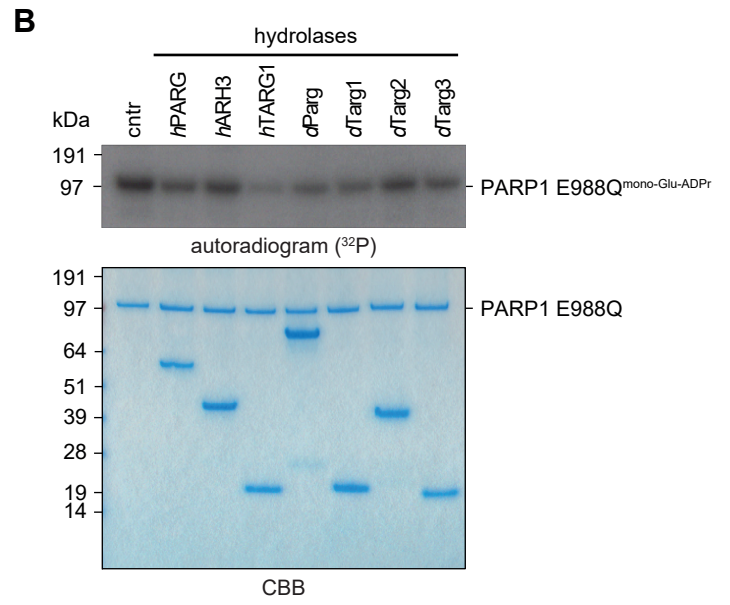
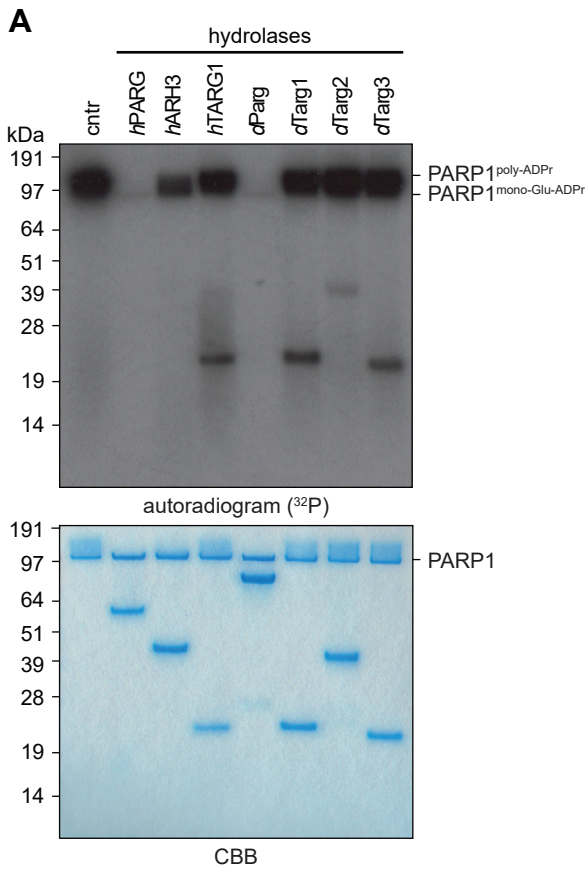


Supplemental Figure 3. MS spectra of *Drosophila* histone H1 and *d*Parp Ser-ADPr sites.

(A-E) Annotated ETD tandem mass spectra of ADP-ribosylated peptides. Full fragmentation is obtained, with both c-ions (blue) and z-ions (red) pinpointing the ADPr to reside on a serine residue. The spectra allowed mapping of the peptides to *Drosophila* histone *d*H1 S199 (A), *d*Parp S363 (B), *d*Parp S491 (C), *d*Parp S494 (D), and *d*Parp S496 (E).

Supplemental Figure 4. Conservation of the PARP automodification domain in insects.

Multiple sequence alignment of selected insect PARP automodification domain sequences. Ser-ADPr sites identified in *dParp* are indicated above the alignment by double-dagger (‡). Indexing indicates *dParp* residue position.



Supplemental Figure 5. Residue specificity of dParg terminal ADPr hydrolase activity.

(A) Removal of poly-Glu-ADPr by human and *Drosophila* (ADP-ribosyl)hydrolases on automodified poly-Glu-*h*PARP1. Poly-Glu-ADPr of *h*PARP1 was achieved by incubation of recombinant *h*PARP1 (0.5 μ M) in the presence of 32 P-NAD⁺ as ADP-ribose donor. The reaction was performed for 30 min at room temperature. The *h*PARP1 reaction was stopped by the addition of 1 μ M olaparib. Lower panel shows the CBB stained SDS-PAGE of the proteins. The experiment was repeated independently three times with similar results.

(B) Removal of mono-Glu-ADPr. Mono-Glu-ADPr was achieved by incubation of recombinant *h*PARP1 E988Q mutant (0.5 μ M) with 32 P-NAD⁺ as ADP-ribose donor and activated DNA. The reaction of *h*PARP1 was stopped by the addition of 1 μ M olaparib and subsequently supplemented with the indicated (ADP-ribosyl)hydrolases. Lower panel shows the CBB stained SDS-PAGE. The experiment was repeated independently three times with similar results.

Multiple sequence alignment for the first region of the protein. It includes species names like Drosophila, Melon fly, House fly, Drosophila bunnanda, Human, Domestic cat, Mouse, Common wombat, C. elegans (PARG1), C. elegans (PARG2), Eye worm, Tetrahymena thermophila, and Monosiga brevicollis MX1. Residue positions 33, 43, 53, 63, 69, 77, and 83 are indicated above the alignment.

Multiple sequence alignment for the second region of the protein. Residue positions 92, 104, 114, 119, 131, and 141 are indicated above the alignment. Species names are consistent with the first region.

Multiple sequence alignment for the third region of the protein. Residue positions 151, 161, 170, 179, 189, 199, 209, and 219 are indicated above the alignment.

Multiple sequence alignment for the fourth region of the protein. Residue positions 229, 238, 248, 258, 268, 278, 286, 296, and 306 are indicated above the alignment.

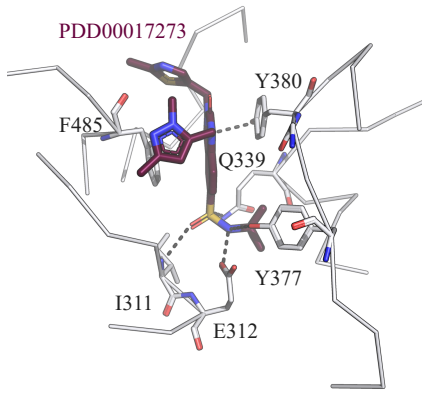
Multiple sequence alignment for the fifth region of the protein, labeled as 'AD-loop 1' and 'AD-loop 2'. Residue positions 316, 326, 336, 346, 356, 365, 375, and 385 are indicated above the alignment. Some residues are boxed in red.

Multiple sequence alignment for the sixth region of the protein, labeled as 'loop 1' and 'Tyr loop'. Residue positions 399, 409, 424, 434, 441, 450, and 460 are indicated above the alignment. Some residues are boxed in red.

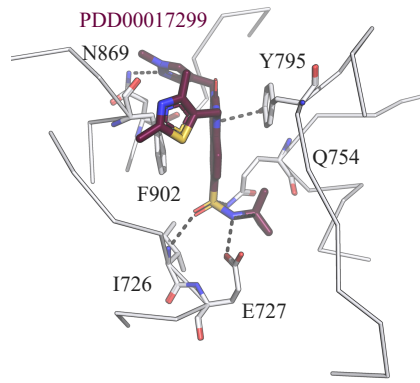
Multiple sequence alignment for the seventh region of the protein, labeled as 'loop 2'. Residue positions 470, 480, 490, 498, 508, 518, 528, 538, and 548 are indicated above the alignment. Some residues are boxed in red.

Supplemental Figure 6. Conservation of PARG within *Animalia*.

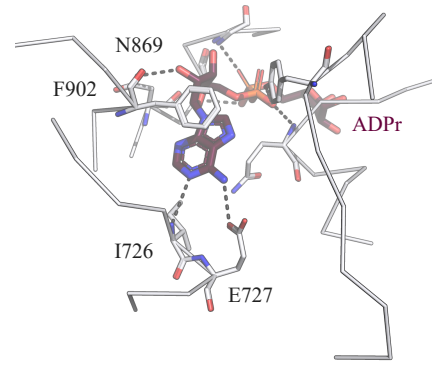
Multiple sequence alignment of the catalytic domain of selected PARG sequences from *Insecta*, *Mammalia*, *Nematoda* and *Protozoa* phyla. The accessory (yellow) and macrodomain (blue) regions are indicated below the alignment and catalytically important regions highlighted by coloured boxes (AD-loop 1 and 2, green; loop 1 and 2, red; Tyr loop, rose). Residues known to be crucial for catalysis are indicated above the alignment by double-dagger (‡) and threonine/leucine residue involved in the loop 1-AD-loop 1 interaction by downward triangle (▼). Indexing indicates *dParp* residue position.



dParg:PARGi (8ADJ)



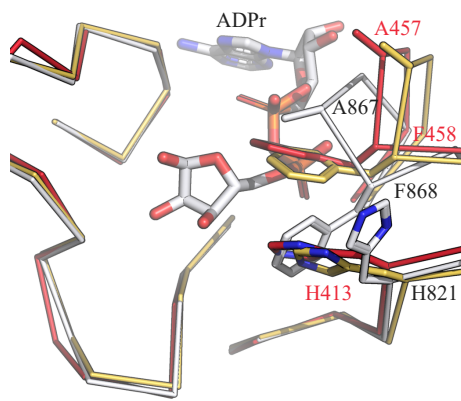
hPARG:PARGi (6HML)



hPARG:ADPr (4B1H)

Supplemental Figure 7. Structure of the *d*Parg:PDD00017273 complex.

Ribbon-liquorice representation of the ligand coordination of the *d*Parg:PDD00017273, *h*PARG:PDD00017299, and *h*PARG:ADP-ribose complexes. Residues important for the protein:ligand interaction are highlighted and numbering corresponds to the respective sequences.



- dPARG apo (8ADK)
- mPARG apo (4FC2)
- mPARG:ADPr (4NA0)

Supplemental Figure 8. Ligand binding involves conformational changes of loop 2.

Ribbon-liquorice representation of loop 2 conformational changes triggered by ligand binding. Residue numbers of *d*Parg are given in red and of *m*PARG in black.